

# Ac conductivity relaxation processes and its scaling behavior in sodium bismuthate glasses

R. MURUGARAJ, G. GOVINDARAJ\*

*Raman School of Physics, Pondicherry University, Pondicherry 605 014, India*

*E-mail: ggraj\_54@lycos.com*

*E-mail: purm72@mailcity.com*

DEEPA GEORGE

*Department of Physics, Rajiv Gandhi College of Engineering and Technology,  
Pondicherry 607 402, India*

Ac conductivity measurements and its analysis has been performed on the glassy ionic conducting  $x \text{Na}_2\text{O} + (1 - x) \text{Bi}_2\text{O}_3$  system in the frequency range from 20 Hz to 1 MHz and in the temperature range 450 K to 750 K. The composition dependence of the dc electrical conductivity and activation energy has been obtained. The electrical relaxation analysis has been inquired on these glasses with universal power law and the random free energy barrier model. The relaxation parameters are obtained from the analysis has been compared. All experimentally known features of the  $\sigma'(\omega)$  including its scaling behavior are explained satisfactorily. The results show an excellent agreement of scaling behavior based on random free energy barrier model and universal power law.

© 2002 Kluwer Academic Publishers

## 1. Introduction

In the review of literatures, ordered solids show no frequency dependence on their conductivity below phonon frequencies, but, disordered solids shows dispersion as a function of frequency. In the last few decades, it has been witnessed that there is a rapid progress of ac conductivity measurements, its analysis and scaling behavior on ionically conducting disordered solids such as ion conducting doped crystals, poly-crystals, ion conducting glasses, amorphous semiconductors, and ion conducting polymers [1–10]. These disordered materials share common features such as: (1) disordered arrangements of the mobile ions within rigid matrix; (2) thermally activated hopping processes of the mobile ions, giving rise to a dc conduction and (3) the remarkable features of ac conductivity and its scaling behavior. The variation of the ac conductivity with frequency commonly takes the form of low frequency region with a constant conductivity, while at higher frequencies the conductivity becomes strongly frequency dependent and increases with frequency up to phonon frequencies. The low frequency plateau is regarded as the dc conductivity. The generality of this dispersive behavior for many classes of materials was pointed out by Jonscher [11, 12]. In all the cases, above the loss peak frequency, ( $\omega > 1/\tau$ ), where  $\tau$  is the relaxation time, the real part of complex conductivity  $\sigma'(\omega)$  and the imaginary part of complex permittivity  $\varepsilon''(\omega)$  are empirically represented as  $\sigma'(\omega) \propto \omega^s$  and  $\varepsilon''(\omega) \propto \omega^{s-1}$ , with  $0 < s < 1$ , respectively. In the

literature there are many approaches have been put forward to explain this observed features [13–17].

In the past few years, it is well known that heavy metal network glass formers such as  $\text{Bi}_2\text{O}_3$ ,  $\text{TeO}_2$ ,  $\text{Ga}_2\text{O}_3$  have received considerable attention for their technological applications. The glasses based on these network formers are good candidates as hosts for optical, electronic and other applications [18–28]. They are also interesting materials for structural and electrical relaxation investigations since they form stable glasses by a conventional melt quenching technique even though none of the constituents is a traditional network glass former. Review of literature shows that optical spectroscopic studies have been carried out extensive on bismuthate glasses with and without doping of transition metal oxides [18–25]. However, there are limited studies on the electrical relaxation characterisation on lithium and copper doped bismuthate glasses both ionic and electronic nature [26–28]. There is no report on the electrical (ionic) relaxation studies on sodium bismuthate glasses.

Therefore, in the present work, the dc conductivity, activation energy and conductivity relaxation process through Cole-Cole type impedance response function in sodium bismuthate glasses is studied as a function of composition and temperature. The observed ac conductivity and its scaling behavior in  $x \text{Na}_2\text{O} + (1 - x)\text{Bi}_2\text{O}_3$  are studied using Jonscher's universal power law and random free energy barrier model [14, 15].

\* Author to whom all correspondence should be addressed.

In the Section 2 preparation, ac electrical measurements, impedance, and conductivity analysis of  $x \text{Na}_2\text{O} + (1-x) \text{Bi}_2\text{O}_3$  glassy system is discussed. Section 3 is on the result and discussion of dc conductivity, ac conductivity and its scaling behavior using Jonscher's universal power law and on random free energy barrier model. The summary and conclusions are dealt in Section 4.

## 2. Experimental

The different composition of the  $x \text{Na}_2\text{O} + (1-x) \text{Bi}_2\text{O}_3$  glassy systems were prepared from reagent grade  $\text{Na}_2\text{CO}_3$  and  $\text{Bi}_2\text{O}_3$  by melt quenching process. The appropriate amount of ingredients are taken in open silica crucible and kept in a furnace for two hours at  $475^\circ\text{C}$  for de-carbonisation and melted for 30 to 50 min at about  $800^\circ\text{C}$  to  $850^\circ\text{C}$  depending on the composition. The melt was then quenched between stainless steel plate kept at room temperature. Since the quenched samples remain brittle, the glasses were pulverised into fine powder and pressed into pellets of 10 mm diameter and about 1 mm thick by applying a pressure of 5000–8000  $\text{Kg}/\text{cm}^2$  for about 15 min using a hand press. The amorphous nature of the samples was confirmed by the peak free pattern of X-ray diffraction spectra obtained from Rigaku X-ray Diffractogram. Further the amorphous nature of the samples were ascertained by thermal analysis using Mettler differential scanning calorimeter at the scanning rate of  $10^\circ\text{C}/\text{min}$ .

Before making ac electrical conductivity measurements, the pellets are annealed at  $200^\circ\text{C}$  for about 18 hours to remove the residual stresses. The ac conductivity measurements carried out in the temperature range from  $200^\circ\text{C}$  to  $500^\circ\text{C}$  by sandwiching these pellets between electrical leads made up of silver. Zentech 3305 component analyzer was used to measure the capacitance  $C_p$  and conductance  $G_p$  in the frequency range from 20 Hz to 1 MHz. Data analysis were made by using electrochemical impedance software Equivalent Circuit (EC) version 3.97 [29] and the sample parameters like bulk conductivity, electrode resistance and electrode capacitance were calculated. Fig. 1 shows the impedance dispersion behavior for the sample  $0.5\text{Na}_2\text{O} + 0.5\text{Bi}_2\text{O}_3$  at 467 K. The impedance spectra shows two depressed semi-circles combined each other. The depressed semi-circles are analysed based on Cole-Cole type [30] impedance response function defined as

$$Z^*(\omega) = Z_\infty + \frac{Z_s - Z_\infty}{1 + (i\omega\tau_m)^{(1-\alpha)}} \quad (1)$$

by non-linear least square fitting. Where  $Z_s$  is the static impedance,  $Z_\infty$  is impedance at high frequency limit,  $\tau_m$  is the mean relaxation time of Cole-Cole distribution of relaxation times and  $\alpha$  is the Cole-Cole exponent lies in the range  $0 < \alpha < 1$ . From Fig. 1, one can see that the electrode-sample interface dispersion is more prominent at low frequency region. The high frequency dispersion is attributed to the sample resistance and its constant phase element,  $Q(j\omega)^{1-\alpha}$ , where  $Q$  is constant phase element,  $j = \sqrt{-1}$ . The frequency disper-

TABLE I The magnitude of Cole-Cole exponent  $\alpha$ , the mean relaxation time  $\tau_m$  and dc conductivity at 467 K and activation energy for the  $x \text{Na}_2\text{O} + (1-x) \text{Bi}_2\text{O}_3$  system

Composition (x)	$\alpha$	$\tau_m$ ( $\text{rad}^{-1}$ )	$\sigma_{\text{dc}}$ at 467 K ( $\text{S cm}^{-1}$ )	$E_{\text{dc}}$ (eV)
0.1	0.02509	$3.1952 \times 10^{-4}$	$4.6862 \times 10^{-7}$	1.05
0.2	0.01880	$1.9919 \times 10^{-4}$	$5.3046 \times 10^{-7}$	1.03
0.3	0.07685	$1.2098 \times 10^{-4}$	$2.0363 \times 10^{-6}$	0.99
0.4	0.04703	$1.9948 \times 10^{-4}$	$6.3404 \times 10^{-7}$	0.94
0.5	0.02600	$3.2031 \times 10^{-5}$	$4.1566 \times 10^{-6}$	0.76

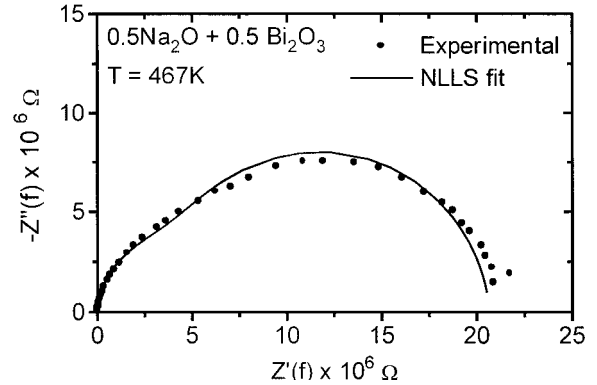


Figure 1 Impedance spectra for the sample  $0.5\text{Na}_2\text{O} + 0.5\text{Bi}_2\text{O}_3$  at 467 K. Dots are experimental points. Continuous line corresponds to Simulated fit.

sion based on the final parameters is compared with the total measured dispersion in the fit quality plot using the dispersion simulation program. In Fig. 1 the continuous line is the fitted curve using the dispersion simulation program. Following the similar procedure for different compositions of the sample at different temperatures are analysed. From the analysis, it is obvious that the high frequency depressed semi-circle do not pass through the origin. This is because the impedance at higher frequency satisfies the condition  $Z_\infty > 0$ , where  $Z_\infty$  is the high frequency limit of impedance. The depressed semicircle below the real axis indicates the presence of distributed elements in the sample and sample-electrode system, which indicates that, the relaxation time is not single valued but it is distributed continuously or discretely around a mean relaxation time  $\tau_m$ . The magnitude Cole-Cole exponent  $\alpha$  and the mean relaxation time  $\tau_m$  for all the samples at 467 K are reported in Table I. Similarly, the magnitude Cole-Cole exponent  $\alpha$  and the mean relaxation time  $\tau_m$  for the sample  $0.4\text{Na}_2\text{O} + 0.6\text{Bi}_2\text{O}_3$  at different temperature are reported in Table II.

## 3. Results and discussion

### 3.1. DC Conductivity and activation energy

The dc resistance at different temperature for all the compositions is obtained from the non-linear least square analysis of complex impedance plots. The dc conductivity of the sample is given by  $\sigma_{\text{dc}} = d/(Ra) \text{S cm}^{-1}$ , where  $d$  is the thickness of the sample in cm,  $a$  is the area of cross section of the sample

TABLE II The magnitude of Cole-Cole exponent  $\alpha$ , the mean relaxation time  $\tau_m$  at different temperature for the sample  $0.4\text{Na}_2\text{O} + 0.6\text{Bi}_2\text{O}_3$

Temperature (K)	$\alpha$	$\tau_m$ (rad <sup>-1</sup> )
467	0.04703	$1.9948 \times 10^{-4}$
514	0.04713	$2.1269 \times 10^{-5}$
567	0.06775	$4.5368 \times 10^{-6}$
614	0.12919	$2.3076 \times 10^{-6}$
668	0.29548	$1.9839 \times 10^{-6}$
712	0.21797	$2.9294 \times 10^{-7}$

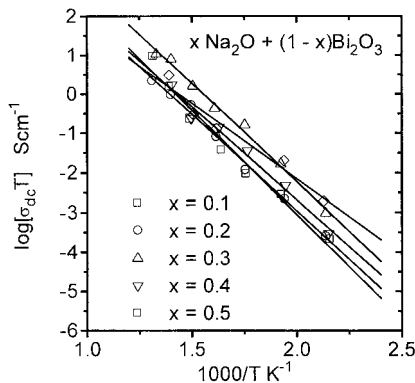


Figure 2  $\log[\sigma_{dc}T]$  versus  $1000/T$  for the glassy system  $x\text{Na}_2\text{O} + (1-x)\text{Bi}_2\text{O}_3$ . Lines are linear least square fit. Symbols are experimental points.

in  $\text{cm}^2$  and  $R$  is the bulk resistance in ohm. The temperature dependence of dc conductivity in the form of  $\log[\sigma_{dc}T]$  versus  $1000/T$  plot for all the composition are shown in Fig. 2. It is found that the dc conductivity increases with increases in temperature and obey the Arrhenius behavior

$$\sigma T = \sigma_0 \exp[-E_{dc}/kT] \quad (2)$$

where  $\sigma_0$  is the pre-exponential factor depends on composition, mobility of diffusion ions, etc.,  $E_{dc}$  is the de activation energy of the samples,  $k$  and  $T$  has the usual meanings. The magnitude of dc conductivity at 467 K and activation energy for all samples are reported in Table I. From the Table I, it is observed that the dc activation energy decreases with increase of alkali oxide indicating that the alkali oxide ( $\text{Na}_2\text{O}$ ) enters in the host glass matrix.

### 3.2. AC Conductivity and scaling analysis

The measured parallel conductance  $G_p$  values were used to study the ac conductivity behavior of prepared samples through the real part of ac conductivity. Fig. 3 shows the typical ac conductivity behavior of the sample  $0.1\text{Na}_2\text{O} + 0.9\text{Bi}_2\text{O}_3$  at different temperature. All samples exhibit the high frequency dispersion with indispensable part of frequency independent conductivity at low frequencies. The switch over from the frequency independent region to frequency dependent region signs the on set of conductivity relaxation, which shift towards higher frequencies as the temperature increases. The simplest and most common explanation for a conductivity which increases with frequency

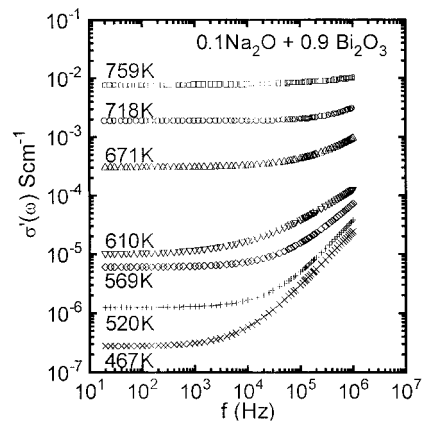


Figure 3  $\sigma'(\omega)$  as a function of frequency for the sample  $0.1\text{Na}_2\text{O} + 0.9\text{Bi}_2\text{O}_3$  at different temperature.

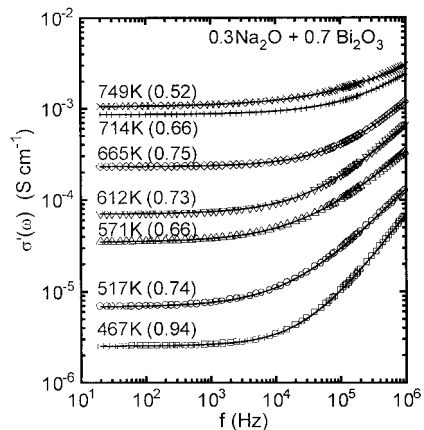


Figure 4  $\sigma'(\omega)$  as a function of frequency for the sample  $0.3\text{Na}_2\text{O} + 0.7\text{Bi}_2\text{O}_3$  at different temperature. Solid lines are the best fits of Equation 3. The magnitude of  $s$  is shown with in the bracket.

is the existence of one or the other kind of inhomogeneities in the solids i.e., a strong frequency dispersion of the conductivity is observed only in disordered solids. The inhomogeneities in the solid may be of a microscopic in nature with the distribution of relaxation processes occurs in disordered solids.

The real part of the ac conductivity of the sample  $0.3\text{Na}_2\text{O} + 0.7\text{Bi}_2\text{O}_3$  shown in Fig. 4 at different temperature. The conductivity spectra shows, that a constant conductivity observes at low frequencies while at high frequencies the conductivity becomes strongly frequency dependent, varying approximately power of the frequency. The ac conductivity relaxation processes in the sodium bismuthate glasses have been analysed using Jonscher's universal power law and random free energy barrier model.

Over large frequency ranges, the conductivity dispersion is well described by the Jonscher's universal power law as [11, 12]:

$$\sigma'(\omega) = \sigma(o) + A\omega^s, \quad 0 < s < 1 \quad (3)$$

where  $\sigma(o)$  is frequency independent conductivity,  $A$  is pre-factor depends on temperature and composition and  $s$  is the frequency exponent. The frequency exponent  $s$  increases as the temperature  $T$  decreases, as for the  $T \rightarrow 0$ , one finds  $s$  equal to one [31].

The frequency exponent  $s$  in Equation 3 is calculated using non linear least square fit procedure of Levenberg-Marquardt [32] for all the samples at different temperatures. The magnitude of  $s$  for the sample  $0.3\text{Na}_2\text{O} + 0.7\text{Bi}_2\text{O}_3$  is shown in Fig. 4 within the bracket. The dots are experimental points and the continuous lines are best fit of Equation 3.

Recently, there has been renewed interest in the scaling and the striking universality of ac data in ionic conductive glasses [1, 3, 7, 33, 34]. It is usually possible to scale the ac data at different temperature and composition into a single master curve. The master curve gives the dimensionless ac conductivity as a function of dimensionless frequency, and it can be referred as time-temperature superposition principle. In the literature, the scaling behavior in ac conductivity is studied either by using Equation 3, or with  $\omega_c$  which is characteristic, but *arbitrarily* determined frequency [33].

In recent publications [1, 3, 7, 33–36], the scaling behavior in ac conductivity has been studied, instead of scaling the ac conductivity by the  $\omega_p$ , the directly accessible quantities such as the temperature, the dc conductivity, ionic concentration and dielectric strength  $\Delta\varepsilon = \varepsilon_s - \varepsilon_\infty$  are used. Roling and his co-workers [35], has studied the scaling in the ac conductivity at different temperature by scaling the frequency axis with (a)  $\omega_c = \sigma(0)T$  (b)  $\omega_c = \sigma(0)T/x$ , where  $x$  depends on the compositions, which takes care of the changes in cation number density. Sidebottom [5, 33, 36], in his recent work, suggested a universal approach for scaling the ac conductivity by defining the  $\omega_c = \varepsilon_0 \Delta\varepsilon / \sigma(0)$ , where  $\Delta\varepsilon = \varepsilon_s - \varepsilon_\infty$ . Some disordered solids do not possess a well defined dielectric loss peaks, and as a consequence the value of the static dielectric constant could not be obtained from the measured frequency dependence dielectric data. Under these circumstances, the frequency axis is scaled with respect to hopping frequency which automatically taken in to account the permittivity change and correlation effects between successive hops in the disordered lattice [7]. Therefore, in the present work, we use the loss peak frequency or hopping frequency  $\omega_p$ , as the scaling frequency for the frequency axis and dc conductivity for the conductivity axis based on Almond-West conductivity formalisms [37–39]. In this formalism the scaling behavior of ac conductivity is obtained from Equation 3 and it is given by

$$\sigma'(\omega) = \sigma(0) \left[ 1 + (\omega/\omega_p)^s \right] \quad (4)$$

where the pre factor  $A = \sigma(0)/\omega_p^s$ .

Fig. 5 shows the real part of the ac conductivity for the sample  $0.3\text{Na}_2\text{O} + 0.7\text{Bi}_2\text{O}_3$  at different temperature is scaled by the respective dc conductivity and hopping frequency with constant  $s = 0.66$ .

There are two basic types of theory that have been used in the literature to describe the universal electrical properties of disordered ionic conductors (Equation 3). In the *first* approach, the ionic hopping events are independent and have a broad distribution of relaxation times through the distribution of energy barriers. In the *second* approach, collective effects occur such that each hopping ion has strong interactions (usually of Coulom-

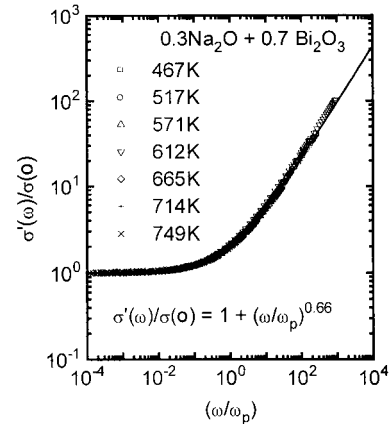


Figure 5  $\sigma'(\omega)/\sigma(0)$  as a function of  $\omega/\omega_p$  for the sample  $0.3\text{Na}_2\text{O} + 0.7\text{Bi}_2\text{O}_3$  at different temperatures. The solid line corresponds to Equation 4 with  $s = 0.66$ .

bic type) with surrounding ions in the disordered lattice. In the literature there are many attempts to justify that the power law Equation 3 has the origin of either distribution of energy barriers or nearest-neighbor coulomb interactions and/or with site energy distribution. Though a complete model for glass ionic conductivity does not exist today, it is seldom questioned that the basic conduction mechanism is thermally activated hopping across an energy barrier, a process described by Eyring's rate theory. The justification of thermally activated hopping models is possible from the fact that both dc and ac conduction are due to the same mechanism with the assumption of jump frequency distribution is that corresponding distribution of free energy barriers for jumps.

In Dyre's random free energy barrier model (RFEBM), it is assumed that the disorderliness is felt through the distribution of jump frequencies with all the jump distances are assumed to be equal and all the free energy barriers are equally likely. Under the framework of continuous time random walk (CTRW) model [40–42] based on Stevel's and Taylor's random potential energy model [43–45] the ac conductivity is given by

$$\frac{\sigma'(\omega)}{\sigma(0)} = \frac{\omega\tau \tan^{-1}(\omega\tau)}{[\ln[\sqrt{1 + \omega^2\tau^2}]]^2 + [\tan^{-1}(\omega\tau)]^2} \quad (5)$$

By Equation 5 one can observe that the dispersion in  $\sigma'(\omega)$  through relaxation time  $\tau$  which is the reciprocal of the minimum jump frequency  $\gamma_{\min}$  for the distribution of energy barriers. In disordered solids, Dyre's random free energy barrier model satisfies all the criteria of ac conductivity and its dispersive behavior. Therefore, in the present work, we study the scaling behavior in ac conductivity based on the minimum jump frequency  $\gamma_{\min} = 1/\tau$  as the scaling frequency and compared with the power law scaling behavior Equation 4. Fig. 6 shows the real part of the ac conductivity for the sample  $0.3\text{Na}_2\text{O} + 0.7\text{Bi}_2\text{O}_3$  at different temperature are scaled by the respective dc conductivity and characteristic frequency  $\omega_c = \gamma_{\min}$  of random free energy barrier model.

The interesting observation in Fig. 5 is that, the scaling curves spreads near and above the hopping

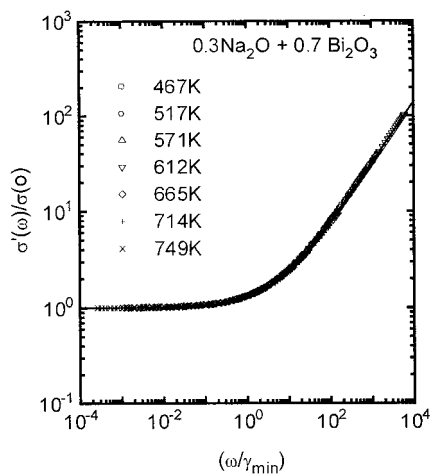


Figure 6  $\sigma'(\omega)/\sigma(0)$  as a function of  $\omega/\gamma_{\min}$  for the sample  $0.3\text{Na}_2\text{O} + 0.7\text{Bi}_2\text{O}_3$  at different temperatures. The solid line corresponds to Equation 6.

frequency when conductivity spectrum is scaled by  $\omega_p$ . However, when the conductivity spectrum is scaled by the  $\omega_c = \gamma_{\min}$ , we found that the  $\sigma'(\omega/\gamma_{\min})/\sigma(0)$  vs  $\log(\omega/\gamma_{\min})$  curves collapse in to a single master curve defined by

$$\frac{\sigma'(v)}{\sigma(0)} = \frac{v \tan^{-1}(v)}{[\ln[\sqrt{1+v^2}]]^2 + [\tan^{-1}(v)]^2} \quad (6)$$

where  $v = \omega/\gamma_{\min}$  is a scaled frequency. In Fig. 6, the continuous line corresponds to Equation 6. In an effort to confirm the generality of the scaling result shown in Figs 5 and 6, the scaling behavior is studied for all different compositions and the results are published elsewhere. In all the cases, we found that the  $\sigma'(\omega/\gamma_{\min})/\sigma(0)$  vs  $\log(\omega/\gamma_{\min})$  curves collapse to a single master curve defined by Equation 6.

From the Figs 5 and 6 the frequency scaling by  $\gamma_{\min}$  on the frequency axis shows better universality of ac conductivity than that of the universal power law scaling. Fig. 7 shows the variation of hopping frequency  $\omega_p$  and the minimum jump frequency of the random free barrier model  $\gamma_{\min}$  for the sample  $0.3\text{Na}_2\text{O} + 0.7\text{Bi}_2\text{O}_3$  at different temperature. From Fig. 7, it is observed that both  $\omega_p$  and the minimum jump frequency  $\gamma_{\min}$  have the same temperature dependence. This suggests that in Jonscher model,  $\omega_p$  which represents the mean of the distribution of the hopping frequencies present in

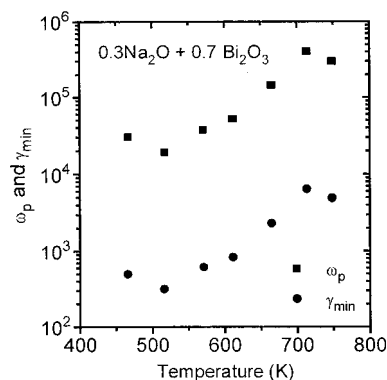


Figure 7 Temperature dependence of loss peak frequency  $\omega_p$  and minimum jump frequency  $\gamma_{\min}$  for the sample  $0.3\text{Na}_2\text{O} + 0.7\text{Bi}_2\text{O}_3$ .

the ionic glasses has the same temperature dependence with that of the minimum jump frequency  $\gamma_{\min}$  in the RFEEM. In Arrhenius representation both  $\omega_p$  and  $\gamma_{\min}$  have the same temperature dependence and have almost same activation energy. In an effort to confirm this generality, the temperature dependence studies on  $\omega_p$  and  $\gamma_{\min}$  for all different compositions has been carried out and the results are in agreement with the above conclusion and the results will be published elsewhere.

#### 4. Summary and conclusions

Sodium bismuthate glasses of different composition were prepared by melt quenching method. Using impedance spectroscopy technique, the measured impedance data are analysed using Cole-Cole type impedance response function. The ac conductivity behavior of sodium bismuthate glasses has been investigated in the frequency range from 20 Hz to 1 MHz and function of temperature. The observed experimental results are discussed based on random free energy barrier model and Jonscher's universal power law. The random free energy barrier model is used to explain the observed dispersive behavior of the ac conductivity in terms of distribution of hopping jump frequencies, which is more fundamental in origin. We have explained the scaling behavior satisfactorily in the ac conductivity by scaling the  $\sigma'(\omega)$  by  $\gamma_{\min}$  than by the loss peak frequency  $\omega_p$ .

#### Acknowledgements

This work is supported under financial assistance of UGC research award scheme 30-64/98/SA-II. One of author (R.M.) is thankful to UGC, Govt. of India for SRF assistance.

#### References

1. J. C. DYRE and T. B. SCHRODER, *Rev. of Mod., Phys.* **72** (2000) 873.
2. K. L. NGAI and C. LEON, *Phys. Rev. B* **60** (1999) 9396.
3. T. B. SCHRODER and J. C. DYRE, *Phys. Rev. Letts.* **84** (2000) 310.
4. D. L. SIDEBOTTOM, P. F. GREEN and R. K. BROW, *ibid.* **74** (1995) 5068.
5. D. L. SIDEBOTTOM, *ibid.* **82** (1999) 3653.
6. J. C. DYRE, *Phys. Rev. B* **49** (1994) 11709; **50** (1994) 9692.
7. A. GHOSH and A. PAN, *Phys. Rev. Letts.* **84** (2000) 2188.
8. A. E. OWEN, *J. Non-Cryst. Solids* **25** (1977) 370.
9. B. ROLLING, *Solid State Ionics* **105** (1998) 185.
10. S. R. ELLIOTT, *ibid.* **70/71** (1994) 27.
11. A. K. JONSCHER, *Nature (London)* **267** (1977) 673.
12. *Idem.*, "Dielectric Relaxation in Solids" (Chelsea Dielectric Press, London, 1983).
13. S. R. ELLIOTT, *Solid State Ionics* **27** (1988) 131.
14. JEPPE. C. DYRE, *J. Non-Cryst. Solids* **135** (1991) 219.
15. *Idem.*, *J. Appl. Phys.* **64** (1988) 2456.
16. K. FUNKE, *Prog. Solid State Chem.* **22** (1993) 111.
17. K. L. NGAI, *Comments Solid State Phys.* **9** (1979) 127; **141** (1980) 141.
18. J. FU and H. YATSUDA, *Phys. Chem. Glasses* **36** (1995) 211.
19. Y. TAKAHASHI and K. YAMAGNEHI, *J. Mater. Sci.* **25** (1990) 3950.
20. Y. B. DIMITRIEV and V. T. MIHAILOVA, *J. Mat. Sci. Letts.* **9** (1990) 1251.
21. A. A. KHARMOLOV, R. M. ALMEIDA and J. HEO, *J. Non-Cryst. Solids* **202** (1996) 233.
22. H. ZHENG, R. XU and J. D. MACKENZIE, *J. Mater; Res.* **4** (1989) 911.

23. D. LEZAL, J. PEDLIKOVA, P. KOSTKA, J. BUDSKA, M. POULAIN and J. ZAVADIL, *J. Non-Cryst. Solids* **284** (2001) 288.
24. GAN FUXI and LIU HUIMIN, *ibid.* **80** (1986) 20.
25. J. FU, *Phys. Chem. Glasses* **37** (1996) 84.
26. J. SWENSON and L. BORJESSON, *Phys. Rev. Letts.* **77** (1996) 3569.
27. A. PAN and A. GHOSH, *J. Chem. Phys.* **112** (2000) 1503.
28. A. GHOSH and D. CHARAVARTHY, *J. Phys.: Condensed Matter* **2** (1990) 931.
29. B. A. BOUKAMP, Equivalent Circuit Version 3.97, Dept. of Chemical Tech. Univ. of Twente, 7500, AE Enschede, Netherlands (1989).
30. J. ROSS MACDONALD (Ed.), Impedance Spectroscopy (John Willey and Sons, New York, 1987).
31. W. K. LEE, J. F. LIU and A. S. NOWICK, *Phys. Rev. Lett.* **67** (1991) 1559.
32. W. H. PRESS, S. A. TEUKOLSKY, W. T. VELLERLING and B. P. FLANNERY, "Numerical Recipes in Fortran" (Cambridge University Press, 1996) p. 678.
33. D. L. SIDEBOTTOM and T. ZHANG, *Phys. Rev. B* **62** (2000) 5503.
34. B. ROLLING and C. MARTINY, *Phys. Rev. Letts.* **85** (2000) 1274.
35. B. ROLING, A. HAPPE, K. FUNKE and M. D. INGRAM, *ibid.* **78** (1997) 2160.
36. D. L. SIDEBOTTOM, B. ROLLING and K. FUNKE, *Phys. Rev. B* **63** (2001) 5068.
37. D. P. ALMOND, G. K. DUNKAN and A. R. WEST, *Solid State Ionics* **8** (1983) 159.
38. D. P. ALMOND and A. R. WEST, *ibid.* **9/10** (1983) 277.
39. *Idem.*, *ibid.* **23** (1987) 27.
40. E. W. MONTROLL and G. H. WEISS, *J. Math. Phys.* **6** (1965) 167.
41. H. SCHER and M. LAX, *Phys. Rev. B* **7** (1973) 4491.
42. T. ODAGAKI and M. LAX, *ibid.* **24** (1981) 5284.
43. J. M. STEVELS, in "Handbuch der Physik," Vol. 20, edited by S. Flugge (Springer, Berlin, 1957).
44. *Idem.*, *J. Phys. (Paris) Colloq.* **46** (1985) C8.
45. H. E. TAYLOR, *J. Soc. Glass Technol.* **41** (1957) 350T; *ibid.* **43** (1959) 124T.

*Received 22 October 2001  
and accepted 16 July 2002*